EXPERIMENTAL AND NUMERICAL INVESTIGATION OF THERMAL PERFORMANCE OF CHANNELS WITH STAGGERED ARRAY-BASED DIMPLES

by

Yong-Hui XIE[a*], Zhong-Yang SHEN[a], Tian-Yuan LIU[a], and Gong-Nan XIE[b]

[a] School of Energy and Power Engineering, Xi'an Jiaotong University, Xi'an, China
[b] Engineering Simulation and Aerospace Computing, School of Mechanical Engineering, Northwestern Polytechnical University, Xi'an, China

Original scientific paper
DOI: 10.2298/TSCI15S1S13X

Numerical simulation coupled with experimental method was carried out to study the flow and heat transfer characteristics in rectangular channel with staggered array-based dimples. The effect of different dimple depths and Reynolds number were investigated using the shear stress transport turbulent model coupled with gamma-theta transition model. The results indicated that heat transfer and flow resistance of the dimpled surface increases with the increase of dimple depth. Moreover, the thermal performance is sensitive to the flow transition. Heat transfer in each single dimple region increases monotonously in the streamwise direction with Reynolds number increasing. Heat transfer characteristics almost remain the same when the flow is under fully laminar or turbulent but increases greatly when the flow is transited from laminar condition to turbulent condition. Besides, the variations of friction coefficients and thermal performance coefficients are quite similar to those of heat transfer enhancement coefficients, which firstly increases then decreases with the increase of Reynolds number. By comparing the experimental and numerical results, it is found that staggered array-based dimples with $\delta/D = 0.2$ was the most effective structure from the aspect of thermal performance.

Key words: *dimple, array-based, flow characteristics, thermal performance, heat transfer characteristics*

Introduction

Nowadays, a wide range of industrial and scientific equipment are in need of good heat transfer enhancement technology involving gas turbine blades, high-pressure disk and cooling of microelectronic components, *etc.* Dimple is a kind of heat transfer enhancement technology with both low penalty in pressure drop and considerable heat transfer enhancement, which has been a common concern of academic field in recent years.

Terekhov *et al.* [1] conducted the experimental investigation on the heat transfer and aerodynamic resistance of a single dimple with sharp and round edge. The heat transfer enhancement of shallow dimple is caused both by auto oscillations generated by the cavity and the increase in the surface of dimple. The channel height effect on heat transfer and friction in a dimpled passage was experimentally studied by Moon *et al.* [2]. Heat transfer enhancement on the dimpled wall was approximately constant at a value of 2.1 times that of a smooth channel in the thermally developed region, while the average relative friction factors range

* Corresponding author; e-mail: yhxie@mail.xjtu.edu.cn

from 1.6 to 2.0. Arrays of hemispheric and tear-drop shaped dimples were adopted and compared by Chyu *et al.* [3] using automated liquid crystal imaging system. Both of the two type dimple arrays induce heat transfer enhancement about 2.5 times their smooth cases, which is comparable to most of the rib turbulator while the pressure losses is just half of that with rib turbulator. The Nusselt number behavior including local and globally-averaged Nusselt numbers on deep dimpled surfaces within a channel was experimentally investigated by Burgess *et al.* [4]. Experimental results further indicated the deep dimples increased in the strengths and intensity of vortices and increases in the magnitudes of 3-D turbulence production and turbulence transport. The effect of inlet turbulent intensity level, dimple depth and shape on the flow, and heat transfer of a dimpled surface was also investigated in [5-8]. The heat transfer augment increases with the dimple depth when the Reynolds number varies from 9540 to 74800 and the local Nusselt number shows slightly decrease as the inlet turbulent intensity increases. Flow structure and enhanced heat transfer in minichannel with dimpled surfaces was firstly studied by Silva *et al.* [9]. The corresponding results showed that the geometry brings a 67% improvement in heat transfer coefficient, and only a 21% increase in pressure penalty when Reynolds number is 500.

Until now, the works about heat transfer enhancement with dimple have been mainly carried out under the condition of turbulent or laminar flow. It is difficult to understand certain mechanisms under the condition of transitional flow which is discussed in this paper. The present study uses air as coolant to investigate the flow and heat transfer in a channel with staggered array-based dimples. The comparison and analysis of both numerical and experimental results will provide the further engineering application for staggered array-based dimples with reference data.

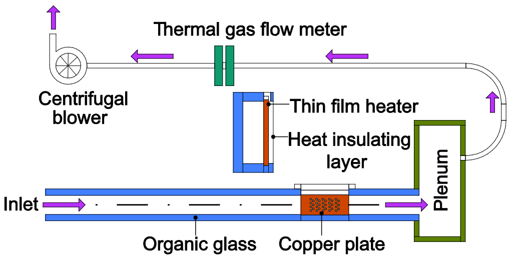

Figure 1. The schematic of experimental facility *(for color image see journal web-site)*

Experimental method

The schematic diagram of the experimental facility used for heat transfer measurements in the present study are shown in fig. 1. The test section consists of four components including an entrance section, a test section, a plenum, and a centrifugal blower section. The entrance section was 80 times the length of the channel height, which could ensure that velocity at the inlet of the test section was fully developed. The channel ahead of the test section is made up of organic glass, and the rest is made up of steel. The plenum was used for stabilizing the air flow. The thermal gas flow meter was set up to measure the mass flow rate. In addition, the centrifugal blower extracting air from the surrounding environment was adjusted to change the experimental Reynolds number. During the test process, constant electrical power is added on the copper plate surface by electrical heater. The steady-state temperature value on copper plate under certain coolant mass flow is recorded by thermocouples which could obtain the heat transfer coefficient data.

Numerical method

Physical model

Staggered array-based dimples were arranged on one side of the channel, and the dimpled surface was shown in fig. 2. There are ten dimple arrays in the streamwise direction as well as thirteen dimple arrays in the cross-section. To get more accurate numerical results, the dimple arrays in the center streamwise direction marked by the dashed line were chosen as the computational domain in fig. 2.

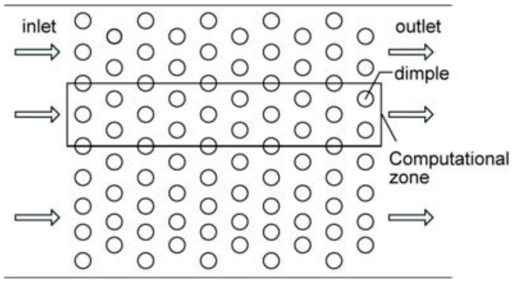

Figure 2. The dimpled surface on the one side of the channel

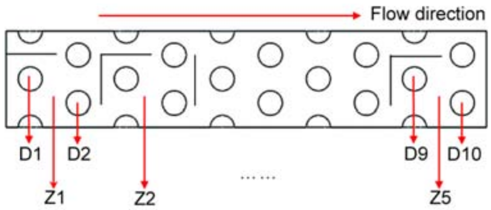

Figure 3. The numbered view of computational region

For boundary conditions, constant heat flux q which was equal to corresponding heat flux in the experiment was applied on the target surface with dimples, and all the walls were no slip in the computation. Periodic boundary conditions were employed on both sides of the dimple arrays, and the wall between target surface and outlet was set as the adiabatic as well as the top wall. The entrance section was established ahead of computational region, and it was 60 times the length of the channel height, which could ensure that velocity at the inlet of the computational region was fully developed. The pressure at outlet and the total temperature at inlet were set as the averaged atmospheric pressure and temperature, 95 kPa and 293 K, respectively. The channel height was set as H/D = 0.5 and the dimple depth δ/D varies from 0.1 to 0.3. In order to conveniently describe the flow and heat transfer performance inside different dimple regions in the streamwise direction, the dimples were numbered successively as D(i), i = 1, …10, and the regions were also numbered successively as Z(i), i = 1, . . . 5, which were shown in fig. 3.

Grid generation and turbulence model

The grid in the whole computational regions was made up of hexahedral elements. O-type grid was applied in dimpled regions for improving the quality of grid and numerical predictions. Near-wall and dimpled surfaces were meshed with fine grids to make sure that y+ is less than 1 in all the involved computational regions as the grid should have a y+ of approximately 1 for capturing the laminar and transition flow in the shear stress transport (SST) turbulence model coupled with gamma-theta transition model. The grid independence validation was performed in the dimpled surface with δ/D = 0.1, Re = 3000. A total of 3174000 finite volume hexahedral cells were employed for the entire target region.

The computational work was carried out by solving the conservation equations of mass, momentum, and energy. The shear stress transport turbulence model coupled with gamma-theta transition model is considered to be a more precise numerical method to solve the transition flow and heat transfer equations in this study. The Navier-Stockes viscous equations solved are shown as:

$$\frac{\partial \rho}{\partial t} + \frac{\partial}{\partial x_i}(\rho u_i) = 0 \tag{1}$$

$$\frac{\partial}{\partial t}(\rho u_i) + \frac{\partial}{\partial x_j}(\rho u_i u_j) = -\frac{\partial p}{\partial x_i} + \frac{\partial \tau_{ij}}{\partial x_j} + \rho \mathrm{g}_i + F_i \tag{2}$$

$$\frac{\partial}{\partial t}(\rho T)+\frac{\partial}{\partial x_j}(\rho u_i T)=\frac{\partial p}{\partial x_i}\left(\frac{k}{c_p}\frac{\partial T}{\partial x_i}\right)+S_T \tag{3}$$

The Nusselt number calculated is defined as:

$$\mathrm{Nu}=\frac{q}{\Delta T}\frac{D_h}{\lambda} \tag{4}$$

The Fanning friction factor f is described as:

$$f=\frac{\frac{\Delta p}{L}D_h}{2\rho u^2} \tag{5}$$

The thermal performance TP is defined as:

$$TP=\frac{\frac{\mathrm{Nu}}{\mathrm{Nu}_0}}{\left(\frac{f}{f_0}\right)^{\frac{1}{3}}} \tag{6}$$

Results and discussion

Flow characteristics

Figure 4 shows the turbulence intermittency contours and the streamline distribution when δ/D = 0.2. The figure shows that the flow is laminar when the turbulence intermittency is near zero as shown in most regions with Re = 1000. The turbulence intermittency in dimpled and corresponding adjacent regions increases with Reynolds number, and the area of laminar flow decreases in the streamwise direction with Re = 3000 and 5000. It is noted that the flow above the dimple D1 starts to transit and the flow in both D6/D10 are similar with Re = 5000 which indicates that the flow is basically fully developed in the streamwise direction from the D6 region. The turbulence intermittency distribution in dimpled and corresponding adjacent regions is similar when Re = 7000. However, the turbulence intermittency distribution is exactly the same and the corresponding value in the most regions is equal to 1 with Re = 9000, which indicates that the flow is fully developed in the whole channel.

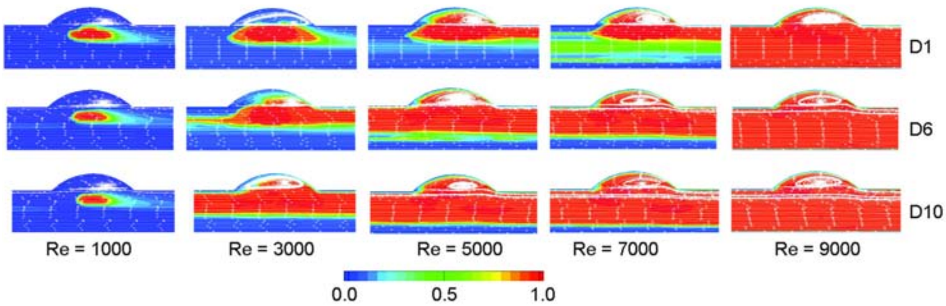

Figure 4. Turbulence intermittency contours and the streamline distribution with δ/D = 0.2
(for color image see journal web-site)

In order to carry out further studies on the characteristics of dimpled regions, fig. 5 shows that the limiting streamline and temperature distributions on dimples Z5 region including D9/D10 target surface. The flow characteristics in the dimples are perfectly symmetrical when δ/D is 0.1 and 0.2, and the limiting streamline and temperature contours show asymmetrical distributions when δ/D = 0.3. The flow separates in the leading edge of the dimple and reattaches in the trailing edge of the dimple in different relative depths. In addition, high temperature regions mainly focus on the first half of dimples.

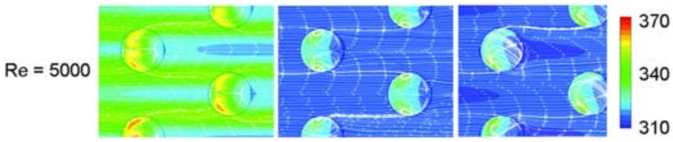

Figure 5. Limiting streamline and temperature distributions on dimple Z5 region (left: δ/D = 0.1, center: δ/D = 0.2, right: δ/D = 0.3) *(for color image see journal web-site)*

Heat transfer and friction characteristics

In order to understand and identify heat transfer characteristics of staggered array-based dimples, experimental study is carried out and compared with the corresponding numerical results. Figure 6 shows the normalized overall averaged Nusselt number variations with Reynolds number. It can be clearly seen that the values of Nu/Nu_0 range from 0.8 to 2.8, and the difference between both numerical and experimental results is not significant. The values of Nu/Nu_0 increase monotonously with the rise of Reynolds number ranging from 1000 to 7000, and heat transfer is enhanced. The values of Nu/Nu_0 ranges from 1 to 1.2 when Re = 9000.

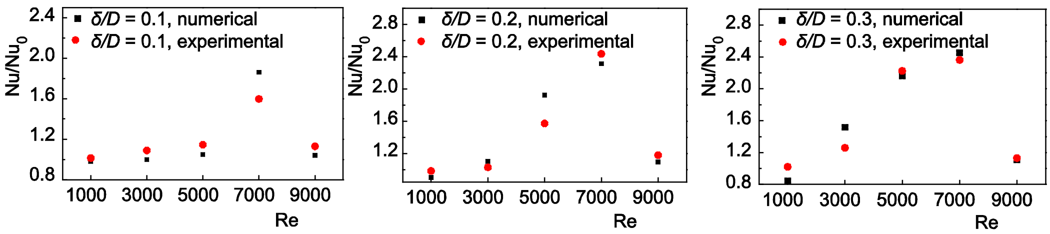

Figure 6. Normalized overall averaged Nusselt number variations with Reynolds number

Figure 7 shows the normalized overall friction factor variations with Reynolds number in order to illustrate the friction characteristics above dimpled surface. It can be seen from fig. 7 that the friction characteristics are similar to heat transfer characteristics of staggered array-based dimples. The values of f/f_0 increase monotonously in most cases with the rise of Reynolds number ranging from 1000 to 7000, and internal resistance losses are increased. The values of f/f_0 decrease sharply when Re = 9000. The normalized overall friction factor ranges from 0.8 to 2.8, which indicates that the friction increases with the enhancement of heat transfer. It can be also seen that the friction increases with the rise of relative depth at the same Reynolds number.

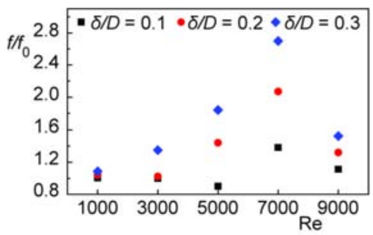

Figure 7. Normalized overall friction factor variations with Reynolds number

Thermal performance

Figure 8 shows the overall thermal performance (*TP*) calculated by both numerical and experimental methods as dependent upon Reynolds number and dimple depths. It can be seen that the thermal performance characteristics are similar with heat transfer and friction characteristics of staggered array-based dimples. The values of *TP* ranging from 0.8 to 2 increase monotonously in most cases with the increasing of Reynolds number from 1000 to 7000 and decrease sharply when Re = 9000, and the differences between numerical and experimental results are very small. The values of *TP* are less than 1 under the condition of laminar flow with different dimple depths, which indicates that thermal performance of dimpled surfaces is worse than that of flat surfaces. It is noted that the differences between the values of *TP* in cases with different dimple depths are obvious when Re = 3000 and Re = 5000, which indicates that transitional flow makes thermal performance sensitive to the variation of dimple depths. As Reynolds number increases, the differences between the values of *TP* ranging from 1.4 to 2 are also obvious when Re = 7000 and thermal performance is the best among all five different Reynolds numbers. When the flow is turbulent, the differences between the values of *TP* ranging from 1 to 1.1 are not significant and the overall thermal performance is not enhanced with large degree, which indicates that transitional flow can effectively improve the overall thermal performance of dimpled surface. In addition, there is an inverse relationship between dimple depth and the values of *TP*.

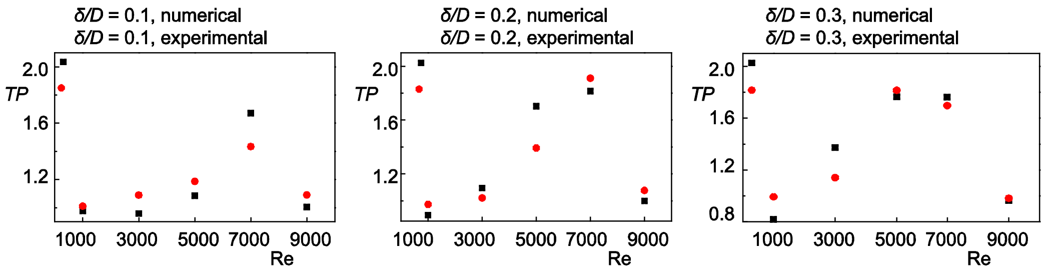

Figure 8. Overall thermal performance variation with Reynolds number

Conclusions

The averaged Nusselt number decreases monotonously along with streamwise direction in different dimple depths under laminar flow and turbulent flow. It firstly decreases then increases along with streamwise direction under transitional flow. The normalized averaged Nusselt number increases monotonously along with streamwise direction. The averaged Nusselt number for each dimple region is lower than and slightly greater than that for the corresponding region in flat cases with different dimple depths under the condition of laminar flow and turbulent flow, which indicates that heat transfer is not enhanced. The transitional flow exhibits better heat transfer performance. The normalized overall averaged Nusselt number increase monotonously with the rise of Reynolds number ranging from 1000 to 7000, and decreases sharply when Re = 9000. The variations of the normalized overall friction factor and the overall thermal performance are similar to those of the normalized overall averaged Nusselt number. The values of *TP* are near one under the condition of laminar flow with different dimple depths, which indicates that thermal performance of dimpled surfaces is worse and that of flat surfaces. The values of *TP* increase with the rise of Reynolds number, and thermal performance of dimpled surfaces enhances significantly. Transitional flow can effectively improve the overall thermal performance of dimpled surface.

The overall thermal performance of staggered array-based dimples which are as high as 1.81 and 1.91 are the best according to numerical and experimental results with $\delta/D = 0.2$ and Re = 7000, respectively. The staggered array-based dimples with $\delta/D = 0.2$ shows the best performance among the transitional flow.

Nomenclature

C_p – specific heat, [$\mathrm{Jkg^{-1}K^{-1}}$]
D_h – hydraulic diameter, [mm]
D – dimple print-diameter, [mm]
F_i – external volume force, [N]
f – friction factor, [–]
g_i – gravity force, [N]
h – heat transfer coefficient, [$\mathrm{Wm^{-2}K^{-1}}$]
L – channel length, [m]
Nu – Nusselt number, [–]
Nu_0 – baseline Nusselt number, [–]
ΔP – pressure drop, [Pa]
q – heat flux, [$\mathrm{Wm^{-2}}$]
Re – Reynolds number, [–]
T – temperature, [K]
TP – thermal performance, [–]
ΔT – mean temperature difference, [K]
u – velocity, [$\mathrm{ms^{-1}}$]

Greek symbols

δ – dimple/protrusion depth, [mm]
λ – thermal conductivity, [$\mathrm{Wm^{-1}K^{-1}}$]
ρ – density, [$\mathrm{kgm^{-3}}$]

References

[1] Terekhov, V. I., *et al.*, Heat Transfer Coefficient and Aerodynamic Resistance on a Surface with a Single Dimple, *Enhanced Heat Transfer*, *4* (1997), 2, pp. 131-145
[2] Moon, H. K., *et al.*, Channel Height Effect on Heat Transfer and Friction in a Dimpled Passage, *Journal of Engineering for Gas Turbines and Power*, *122* (2000), 2, pp. 307-313
[3] Chyu, M., *et al.*, Heat Transfer Enhancement in Rectangular Channels with Concavities, *Enhanced Heat Transfer*, *6* (1999), 6, pp. 429-439
[4] Burgess, N. K., *et al.*, Nusselt Number Behavior on Deep Dimpled Surfaces within a Channel, *Journal of Heat Transfer*, *125* (2003), 1, pp. 11-18
[5] Ligrani, P. M., *et al.*, Nusselt Numbers and Flow Structure on and above a Shallow Dimpled Surface within a Channel Including Effects of Inlet Turbulence Intensity Level, *Journal of Turbomachinery*, *127* (2005), 2, pp. 321-330
[6] Burgess, N., Ligrani, P. M., Effects of Dimple Depth on Channel Nusselt Numbers and Friction Factors, *Journal of Heat Transfer*, *127* (2005), 8, pp. 839-847
[7] Won, S. Y., *et al.*, Comparisons of Flow Structure above Dimpled Surfaces with Different Dimple Depths in a Channel, *Physics of Fluids*, *17* (2005), 4, pp. 1-9
[8] Won, S. Y., *et al.*, Flow Characteristics along and above Dimpled Surfaces with Three Different Dimple Depths within a Channel, *Journal of Mechanical Science and Technology*, *21* (2007), 11, pp. 1901-1909
[9] Silva, C., E., *et al.*, Flow Structure and Enhanced Heat Transfer in Channel Flow with Dimpled Surfaces: Application to Heat Sinks in Microelectronic Cooling. *Journal of Electronic Packaging*, *129* (2007), 2, pp. 157-166

Paper submitted: November 15, 2014
Paper revised: February 2, 2015
Paper accepted: March 5, 2015